

# Integrated Proteomic Analysis of Major Isoaspartyl-Containing Proteins in the Urine of Wild Type and Protein L-Isoaspartate O-Methyltransferase-Deficient Mice

Shujia Dai,<sup>†</sup> Wenqin Ni,<sup>†,‡</sup> Alexander N. Patananan,<sup>§</sup> Steven G. Clarke,<sup>§</sup> Barry L. Karger,<sup>\*,†,‡</sup> and Zhaohui Sunny Zhou<sup>\*,†,‡</sup>

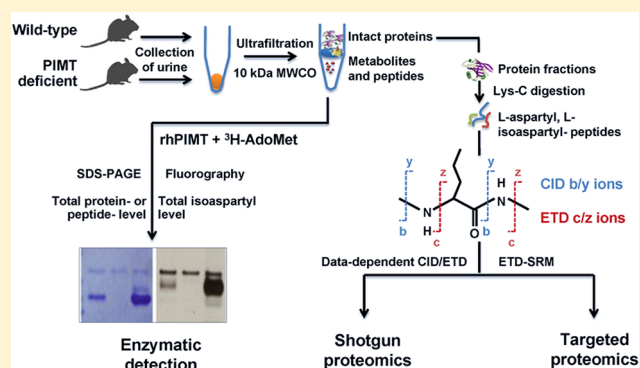
<sup>†</sup>Barnett Institute of Chemical and Biological Analysis, Northeastern University, Boston Massachusetts 02115, United States

<sup>‡</sup>Department of Chemistry and Chemical Biology, Northeastern University, Boston Massachusetts 02115, United States

<sup>§</sup>Department of Chemistry and Biochemistry and the Molecular Biology Institute, University of California, Los Angeles, Los Angeles, California 90095, United States

## Supporting Information

**ABSTRACT:** The formation of isoaspartyl residues (isoAsp or isoD) via either aspartyl isomerization or asparaginyl deamidation alters protein structure and potentially biological function. This is a spontaneous and nonenzymatic process, ubiquitous both *in vivo* and in nonbiological systems, such as in protein pharmaceuticals. In almost all organisms, protein L-isoaspartate O-methyltransferase (PIMT, EC2.1.1.77) recognizes and initiates the conversion of isoAsp back to aspartic acid. Additionally, alternative proteolytic and excretion pathways to metabolize isoaspartyl-containing proteins have been proposed but not fully explored, largely due to the analytical challenges for detecting isoAsp. We report here the relative quantitation and site profiling of isoAsp in urinary proteins from wild type and PIMT-deficient mice, representing products from excretion pathways. First, using a biochemical approach, we found that the total isoaspartyl level of proteins in urine of PIMT-deficient male mice was elevated. Subsequently, the major isoaspartyl protein species in urine from these mice were identified as major urinary proteins (MUPs) by shotgun proteomics. To enhance the sensitivity of isoAsp detection, a targeted proteomic approach using electron transfer dissociation-selected reaction monitoring (ETD-SRM) was developed to investigate isoAsp sites in MUPs. A total of 38 putative isoAsp modification sites in MUPs were investigated, with five derived from the deamidation of asparagine that were confirmed to contribute to the elevated isoAsp levels. Our findings lend experimental evidence for the hypothesized excretion pathway for isoAsp proteins. Additionally, the developed method opens up the possibility to explore processing mechanisms of isoaspartyl proteins at the molecular level, such as the fate of protein pharmaceuticals in circulation.



The generation of isoaspartyl residues in proteins is one of the most common spontaneous, nonenzymatic post-translational modifications. Asparaginyl deamidation and aspartyl isomerization both lead to the generation of the isoaspartyl residue (isoAsp or isoD) as shown in Scheme 1.<sup>1,2</sup> Isoaspartyl residues contain an additional methylene group in the polypeptide backbone, resulting in a  $\beta$ -peptide linkage. As such, the  $\beta$  linkage can impart protein structural changes (kinks) that typically lead to alteration in protein function.<sup>2,3</sup> Proteins containing isoAsp have been associated with the loss of function during aging,<sup>2,4,5</sup> e.g., calmodulin and tubulin in aged brain<sup>6,7</sup> and  $\beta$ -amyloid in Alzheimer's disease.<sup>8,9</sup> Additionally, differences in the proteolytic degradation of isoaspartyl versus aspartyl peptides in antigen-presenting cells may render such peptides immunogenic.<sup>10</sup> IsoAsp formation can also confer specific biological functions, such as in the regulation of the Bcl-2 protein family following DNA damage and cancer

therapy.<sup>11</sup> Additionally, isoAsp has been observed in protein therapeutics and vaccines during production, storage, and even after administration,<sup>12</sup> including tissue plasminogen activator<sup>13</sup> and monoclonal antibodies.<sup>14,15</sup> This modification can alter the immunogenicity and efficacy of the biopharmaceutical.<sup>10,16</sup>

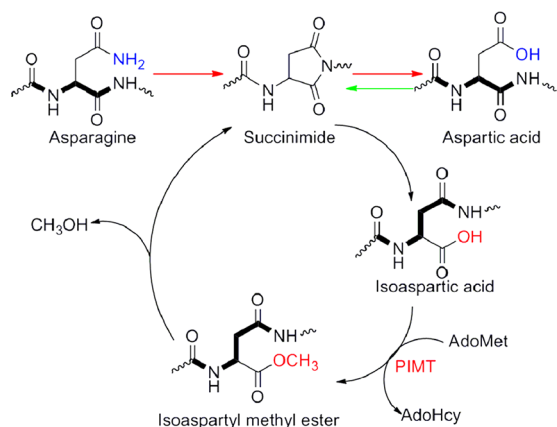
One well-established pathway for isoAsp processing involves the protein L-isoaspartate O-methyltransferase (PIMT or PCMT, EC 2.1.1.77). Using S-adenosylmethionine (AdoMet or SAM), the PIMT enzyme specifically methylates isoAsp,<sup>17</sup> but neither Asp nor Asn, to form methyl isoaspartate ester that ultimately converts back to aspartic acid (see Scheme 1).<sup>18</sup> The overexpression of PIMT extends the lifespan of *Drosophila*<sup>19</sup> and *Escherichia coli*<sup>20</sup> under stress conditions. Conversely, levels

Received: November 26, 2012

Accepted: January 17, 2013

Published: January 17, 2013

**Scheme 1. Formation of isoAsp via Deamidation of Asparagine or Isomerization of Aspartic Acid and the Repair of isoAsp by PIMT<sup>a</sup>**



<sup>a</sup>The peptide backbone is highlighted in bold.

of isoAsp in different cells and tissues in PIMT knockout (KO) mice are significantly elevated over that of the wild-type mice but eventually plateau with age. However, isoaspartyl levels in the urine continue to increase in knockout animals with age, suggesting the existence of alternative proteolytic and excretive isoAsp processing pathways.<sup>21,22</sup> The elucidation of these pathways may not only lead to a better understanding of isoaspartyl regulation but also to potential new approaches for treatment of diseases. However, technical challenges associated with the identification and quantitation of isoAsp have hindered progress in these areas. To overcome these challenges, we report a novel workflow for the proteomic analysis of isoAsp containing proteins in mouse urine, followed by their targeted site-specific quantitation.

The analysis of isoAsp remains difficult due to the subtle differences among isoAsp, Asp, and Asn residues. For example, isoAsp and Asp have identical mass. Enzymatic,<sup>8,23,24</sup> chemical,<sup>25–28</sup> and chromatographic methods<sup>29</sup> have been developed for the detection of isoAsp residues in proteins. In recent years, liquid chromatography–tandem mass spectrometry (LC–MS/MS) has become the method of choice.<sup>30,31</sup> Importantly, the more recent development of electron capture dissociation (ECD)<sup>32</sup> and electron transfer dissociation (ETD)<sup>33–35</sup> make it possible to directly identify isoAsp peptides and their sites. In these methods, isoaspartyl, but not aspartyl residues, can generate site-specific reporter ions,  $c_{l-n} + 57$  ( $C_2H_2O_2$ ) and  $z_n^* - 57$  ( $C_2HO_2$ ) fragments, where  $n$  is the position of the isoAsp residue from the C-terminus of the peptide and  $l$  is the peptide length.<sup>32,33</sup> As a result, LC–MS/MS, using ECD or ETD fragmentation, can differentiate and quantitate Asp and isoAsp residues in peptides.<sup>32</sup> However, for large scale isoAsp analysis using a shotgun proteomics strategy, the specificity and sensitivity of detection by ECD or ETD MS remain inadequate.<sup>36</sup> For example, the MS/MS spectra are commonly acquired in a data-dependent mode in shotgun proteomics, and the randomly selected MS/MS scans do not ensure that fragmentation of precursor ions occurs at or close to the chromatographic peak apex. Therefore, poor sensitivity of isoAsp detection, low quality of MS/MS spectra, and missed identification of peptides can result.<sup>37,38</sup> On the other hand, once candidate isoAsp peptides are identified, ETD/ECD can be fine-tuned to give higher quality data for confirmation.

In this paper, we describe an integrated proteomics workflow to investigate specific isoAsp containing proteins in mice urine. First, using an enzymatic assay based on PIMT, the total isoaspartyl level of proteins in the urine of PIMT-deficient mice was found to be elevated. Subsequently, to identify the major content of excreted isoaspartyl-containing protein species in the urine of wild type (WT) and PIMT knockout mice, proteomic analysis was first performed. On the basis of the results, the digested peptides of a family of major urinary proteins (MUPs) that could potentially form isoAsp were selected for subsequent targeted analysis. Selected reaction monitoring (SRM) with full-scan ETD MS/MS (ETD-SRM) was implemented to enhance the sensitivity of detection of low abundance isoAsp peptides.<sup>35</sup> Five isoaspartyl sites in MUPs were identified and their relative abundance determined. The targeted results indicated higher levels of isoAsp in the urine of PIMT-knockout mice than their wild type littermates, in agreement with the overall isoAsp content in urine, determined separately by an enzymatic method. As a complement to shotgun proteomics, the ETD-SRM targeted approach is demonstrated to generate reliable identification and significantly enhanced sensitivity for quantification for low abundance isoAsp/Asp peptides. The targeted method for isoAsp peptides can be applied as a high throughput assay for the determination of isoAsp modifications in low abundance on proteins in biological fluids.

## ■ EXPERIMENTAL SECTION

**Materials.** Mass spectrometric grade lysyl endopeptidase (Lys-C) was purchased from Wako (Richmond, VA) and <sup>18</sup>O-water (97%) from Cambridge Isotope Laboratories (Andover, MA). LC–MS grade water was obtained from J. T. Baker (Phillipsburg, NJ) and HPLC grade acetonitrile from Thermo Fisher Scientific (Fairlawn, NJ). Amicon ultrafiltration devices, Ultrafree-0.5, with 5 kDa or 10 kDa molecular weight cutoff were obtained from Millipore (Billerica, MA). All other reagents were from Sigma-Aldrich (St. Louis, MO).

**Wild Type and PIMT Knockout Mice and Urine Collection.** PIMT<sup>-/-</sup> mice of a background of 50% C57BL/6J and 50% 129/SvJae were generated from breeding heterozygous PIMT<sup>±</sup> mice.<sup>39</sup> Mice were fed an NIH-31 Modified Diet No. 7013 (Teklad Diets, Madison, WI) and maintained on a 12-h light/dark cycle in a barrier facility. Genotypes were determined by PCR of genomic DNA from tail biopsies of 18-day old pups. The WT primers (5'-ACCCTC-TTCCCATCCACATCGCCGAG and 5'-AGTGGCAGC-GACGGCAGTAACAGCGG), upstream and downstream of exon 1, yield a product of 409 nucleotides in the absence of the neomycin cassette. The KO primers (5'-CGCATCGAGCGA-GCAGTACTCGG and 5'-GCACGAGGAAGCGGTCAG-CCCATT) are both specific for the neomycin resistance gene that is inserted within exon 1, yielding a product of 310 nucleotides. Mouse urine was collected on Parafilm and stored at -20 °C.

**Urine Fractionation Procedure.** Approximately 100  $\mu$ L of mouse urine from WT or KO mice (male or female, three of each group) was applied to a Millipore Amicon Ultra-0.5 centrifugal filter device with a 10 kDa molecular weight cut off and centrifuged at 14 000g for 15 min. The filtrate, representing the peptide fraction, was collected and designated “<10”. To collect the retentate (~40  $\mu$ L), the filter was inverted, placed in a centrifuge tube, and spun for 2 min at 1 000g. The recovered sample (~35  $\mu$ L) contained proteins above approximately 10

kDa, (designated “>10”). Residual small molecules were depleted by adding 5  $\mu\text{L}$  of this material to 245  $\mu\text{L}$  of 0.2 M Bis-Tris (2-[Bis(2-hydroxyethyl)amino]-2-(hydroxymethyl)-1,3-propanediol) buffer (minimum 98% titration), adjusted to pH 6.4 with HCl. After thorough mixing, 225  $\mu\text{L}$  of the sample was applied to a new Amicon filter and centrifuged at 14 000g for 15 min, leaving about 40  $\mu\text{L}$  of retentate. The filter was transferred to a new centrifuge tube, inverted, and centrifuged for 2 min at 1 000g to recover the protein fraction in a volume of about 35  $\mu\text{L}$ .

**Quantitation of Isoaspartyl Content in Mouse Urine.** A plasmid encoding the recombinant human L-isoaspartyl protein methyltransferase (rhPIMT) with an N-terminal polyhistidine tag was a generous gift of Dr. Bruce Downie.<sup>40</sup> The rhPIMT was purified using a His-Trap nickel column (GE Healthcare, Waukesha, WI) and FPLC (BioRad Biologic HR workstation, Hercules, CA) to a concentration of 0.86 mg/mL and a specific activity of 5039 pmol of methyl groups transferred/mg/min. For quantitation, isoAsp residues in whole urine, as well as in the peptide (<10 kDa) and protein (>10 kDa) fractions, were labeled with rhPIMT and S-adenosyl-[methyl-<sup>3</sup>H]-L-methionine ([<sup>3</sup>H]AdoMet; PerkinElmer Inc., 78.0 Ci/mmol, 0.55  $\mu\text{Ci}/\mu\text{L}$  in 10 mM H<sub>2</sub>SO<sub>4</sub>-ethanol (9:1)). Specifically, 5  $\mu\text{L}$  of sample was incubated with 5  $\mu\text{L}$  of rhPIMT, 5  $\mu\text{L}$  of [<sup>3</sup>H]AdoMet (0.35  $\mu\text{M}$  final concentration), and 85  $\mu\text{L}$  of 0.2 M Bis-Tris, pH 6.4 at 37 °C. After a 2 h incubation, 15  $\mu\text{L}$  of the reaction was mixed with 15  $\mu\text{L}$  of 2 $\times$  sodium dodecyl sulfate-polyacrylamide gel electrophoresis (SDS-PAGE) loading buffer (100 mM Tris-HCl, pH 6.8, 200 mM 2-mercaptoethanol, 4% SDS, 20% glycerol, and 0.1% bromophenol blue) and heated for 3 min at 100 °C. SDS gel electrophoresis was performed by loading 25  $\mu\text{L}$  of sample onto a NuPAGE Novex Bis-Tris 4–12% Mini Gel (Invitrogen, Carlsbad, CA) in a running buffer of 50 mM MES, 50 mM Tris base, 0.1% SDS, 1 mM EDTA at pH 7.3 (NuPAGE MES SDS running buffer NP0002). The samples were separated by electrophoresis for approximately 35 min at 200 V, and the gel was stained with Coomassie Brilliant Blue R-250. To identify the isoAsp species, fluorography was performed on the gel by soaking the gel for 1 h with EN<sup>3</sup>HANCE (PerkinElmer, Waltham, MA) after destaining, and incubating the gel for 30 min in water. The gel was subsequently dried for 3 h at 80 °C before being exposed to the film.

**Proteolytic Digestion.** Prior to LC–MS, urinary proteins from WT or KO mice were separately isolated by ultrafiltration (10 kDa MW cutoff) and denatured with 6 M guanidine hydrochloride in 50 mM ammonium bicarbonate, reduced with 10 mM dithiothreitol (DTT) for 30 min at 37 °C, and then alkylated with 20 mM iodoacetamide (IAA) in the dark for 30 min at room temperature. The solvent was exchanged to the digestion buffer (50 mM ammonium bicarbonate, pH 8.3) by centrifuging at 10 000g for 10 min for three cycles in a Millipore Ultrafree-0.5 ultrafiltration device (5 kDa cutoff). The sample was then digested with Lys-C at an enzyme–protein ratio of 1:50 (w/w) at 28 °C for 12 h and next frozen at –80 °C to quench the digestion and minimize any potential deamidation. To investigate the level of deamidation and isomerization induced by the sample preparation process, a duplicate experiment was conducted in parallel following the above same procedure except that <sup>18</sup>O-water and longer incubation times for digestion were investigated.

**LC–MS Analysis.** LC–MS experiments were performed on an LTQ-Orbitrap XL mass spectrometer (Thermo Fisher, San

Jose, CA) equipped with an ETD ion source. An Ultimate 3000 nanoLC pump (Dionex, Mountain View, CA) was used to generate the gradient, and a self-packed reversed phase column (Vydac C18, 300 Å pore size, 5  $\mu\text{m}$  particle size, 75  $\mu\text{m}$  i.d.  $\times$  10 cm, Grace, Deerfield, IL) was coupled online to the mass spectrometer through a Digital PicoView nanospray source (New Objective, Woburn, MA). Mobile phase A consisted of 0.1% formic acid in water and mobile phase B of 0.1% formic acid in acetonitrile. Initially, a linear gradient from 2% to 10% mobile phase B over 2 min and then from 10% to 40% mobile phase B over 90 min was used to separate the digested mixtures at a flow rate of 200 nL/min. At least three blank runs were conducted to minimize any carryover effects between sample injections. The temperature of the ion transfer tube of the linear ion trap was set at 245 °C and the electrospray voltage at 2.2 kV. The mass spectrometer was operated in the data-dependent acquisition mode, switching automatically between one full MS scan at the mass range of 400–2000  $m/z$  and sequential CID MS/MS scans for the nine most abundant precursor ions with a 3.0 mass unit isolation width. Dynamic exclusion was implemented with 2 repeat counts (repeat duration of 30 s, exclusion list 200, and exclusion duration of 30 s). The normalized collision energy for CID was set at 28%. The chemical ionization (CI) source parameters for fluoranthene, such as ion optics, filament emission current, anion injection time (anion target value set at  $3 \times 10^5$  ions), fluoranthene gas flow, and CI gas flow, were optimized automatically, following the standard procedure for tuning the instrument. The time of the ion/ion reaction was maintained constant throughout the experiment at 150 ms. The supplemental activation function was integrated into the ETD data acquisition method, with the collision energy optimized based on the measured charge state of precursor ion. A list of peptides that contain asparagine or aspartic acid was generated from the survey shotgun proteomics. The multiply charged precursor ions that are favorable to ETD fragmentation were then selected for targeted proteomic analysis. Briefly, a full MS scan with resolution 30 000 (at 400  $m/z$ ) in the Orbitrap MS, followed by targeted full-scan ETD MS/MS events in the ion trap MS, was applied to acquire MS and ETD MS/MS spectra of selected precursors.

**Data Processing.** LC–MS/MS data were analyzed using the Xcalibur 2.0.7 software (Thermo Fisher). All files were searched against the mouse SwissProt annotated database (updated in June 2011) using the Sequest algorithm in Proteome Discover 1.2 (Thermo Fisher). Cysteine carbamidomethylation was included as a fixed modification. Deamidation of asparagine was set as a variable modification, and the deamidated residues were assigned based on the +0.984 Da mass shift compared to that of the native form. Full Lys-C enzyme specificity was applied with up to two missed cleavage sites. Mass tolerances were set at 1 Da or 10 ppm for the precursor ions generated in the ion trap or Orbitrap-MS, respectively, and 1.0 Da for the fragment ions in the ion trap. For MS<sup>2</sup> spectral assignment, a false discovery rate (FDR %) of less than 1% at the peptide level was targeted by applying the target-decoy database searching strategy.<sup>41</sup> For all potential isoAsp containing peptides from targeted proteins, ETD-MS<sup>2</sup> spectra and extracted ion chromatograms were manually investigated to confirm the occurrence of isoAsp and its site. Multiple criteria were manually applied as described in the Results and Discussion. Among the multiply charged ions of a given peptide, the precursor with the highest intensity was used

to extract the chromatographic peak area with a 1.0-Da extraction window in the full MS scan. The peak areas from the extracted ion chromatographs (XICs) were then employed to estimate the relative amounts of the Asn, Asp, and isoAsp isoforms.

## RESULTS AND DISCUSSION

### Secreted Proteins/Peptides in Urine of PIMT-Knockout Mice Contain Significant and Elevated Amounts of

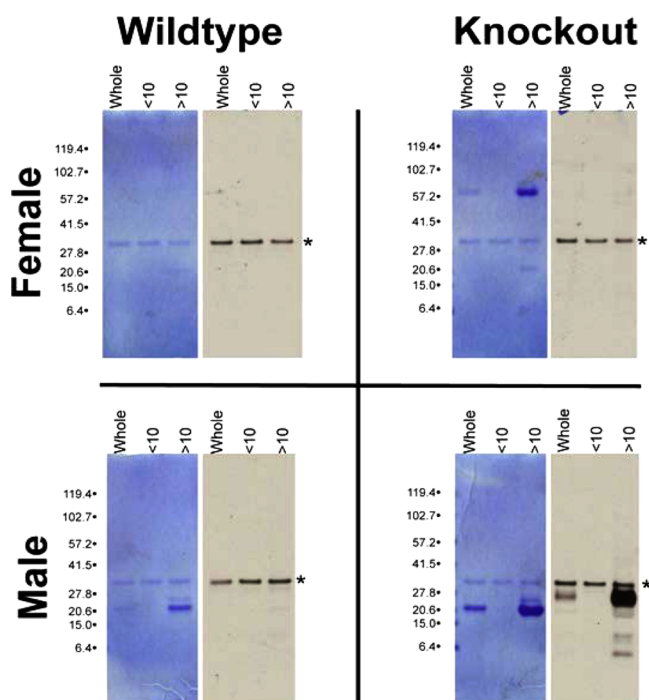


**Figure 1.** Enzymatic detection of isoAsp in mouse urinary species via PIMT-catalyzed methylation followed by fluorography of  $^3\text{H}$ -methyl ester after SDS-PAGE. Isoaspartyl groups in unfractionated (whole) urine were compared to fractionated urine with species less than 10 kDa (<10; peptide fraction) and greater than 10 kDa (>10; protein fraction). The samples were labeled with  $^3\text{H}$ -methyl groups from  $^3\text{H}$ -AdoMet catalyzed by rhPIMT and separated by SDS-PAGE. The dried and EN $^3$ HANCED Coomassie-stained gel is shown on the left, and the fluorograph on the right (82 day exposure at  $-80^\circ\text{C}$  using Kodak BioMax XAR film). The asterisk (\*) denotes the position of automethylated rhPIMT.

**isoAsp.** The total isoAsp levels of the peptide (<10 kDa) and protein (>10 kDa) content in mouse urine were determined by enzymatic labeling coupled with SDS-PAGE, as described previously.<sup>39</sup> As shown in Figure 1, judged by Coomassie staining, proteins at 21 kDa in male urine and 66 and 21 kDa in female urine appeared to be the dominant proteins. On the basis of autoradiography, for the urine of wild type male and female mice or PIMT knockout female mice, only small amounts of methylated protein species (i.e., isoAsp content) were observed at slightly higher than the background level. In comparison, significantly elevated isoAsp levels in urine proteins from PIMT-knockout male mice were observed, as shown in Figure 1 (bands with apparent molecular weight of 27, 21, and 11 kDa, respectively). All of these species were concentrated in the protein fraction of the urine (excretion fraction, > 10 kDa) as compared with the peptide fractions (degradation fraction, <10 kDa) or the unfractionated urine.

The overall changes in isoAsp amount were consistent with our previous results.<sup>20</sup> However, for the first time, the peptide and protein fractions were analyzed separately in this work. The data strongly suggest that both excretion (intact isoaspartyl-containing proteins) and proteolysis (degraded peptides, followed by excretion) are operative in the removal of isoAsp species from circulation in mice. Since the excretion of intact damaged proteins was significantly elevated in knockout male mice, we focused on the fraction of urinary proteins (>10 kDa) from male mice (WT or KO) and applied our proteomics workflow to identify isoAsp-containing proteins, their modification sites, and relative amounts (see Scheme 2).

**Proteomic Analysis of Mouse Urine Proteins.** As described in the Experimental Section, urine protein fractions (>10 kDa) from WT or KO male mice were digested with Lys-C. A nonbiased proteomic analysis with data-dependent CID scans was first performed to identify proteins in mouse urine. Injection of approximately 5  $\mu\text{g}$  of the Lys-C digest into the nanoLC column (the maximum loading amount) led to the identification of 26 proteins with at least two unique peptides. These proteins mainly were soluble proteins from epithelial cell secretion, such as epidermal growth factor (EGF), sulfated glycoprotein 1 (SAP), and kallikrein-1 (KLK1), or from glomerular filtration of plasma proteins, such as major urinary proteins (MUPs) and albumin (ALBU).<sup>42,43</sup>

The top five proteins identified belong to the mouse MUP family, including MUP1, MUP2, MUP3, MUP6, and MUP8 (see Table SI-1 in the Supporting Information) with sequence coverage ranging from 54% to 98%. MUPs are a group of low molecular weight ( $\sim 21$  kDa) secreted proteins produced mainly in the liver<sup>44</sup> that are abundant in the urine and other secretions of many mammals, especially males.<sup>45,46</sup> On the basis of (a) the dominance of MUPs in male mouse urine and (b) the elevated isoAsp level at the 21 kDa protein band in urine from KO male mice, we next targeted MUP species in male urine for comprehensive isoAsp analysis.

**Mapping of isoAsp Sites in MUPs by ETD-SRM Analysis.** To further investigate isoAsp in MUPs, a sensitive and targeted strategy was developed. SRM with ETD MS/MS (ETD-SRM) was implemented based on a full-scan MS with high resolution in the Orbitrap, followed by selected full-scan ETD MS/MS in the ion trap to continuously acquire MS and ETD MS/MS spectra of MUP peptides. Asn- or Asp-containing peptides in MUPs (found in the above proteomic experiment), representing all possible peptide sequences that could contribute to isoAsp formation were selected, and their precursor mass and retention time were employed to establish SRM scanning events. In our study, peptides with only singly charged ions, very short peptide fragments (<5 amino acid residues), miscleaved peptides by Lys-C, and sequence-redundant peptides were excluded from the SRM assay. Those candidate peptides that can generate triply (or higher) charged precursor ions are preferred for the ETD-SRM method. On the basis of these criteria, 13 candidate peptides were selected (see Table SI-2 in the Supporting Information), with 38 Asn or Asp residues, i.e., potential sites for deamidation and/or isoaspartyl isomerization.

A 90 min LC-MS gradient was divided into several time-based segments. The SRM data-acquisition window for each precursor was set at 10 min, based on the retention time of the selected unmodified peptide. The baseline separation of the deamidation products ensured the purity of the ETD spectra, thus minimizing the potential interference from other isoAsp

## Scheme 2. Integrated Proteomic Workflow of Major isoAsp Proteins in Mouse Urine

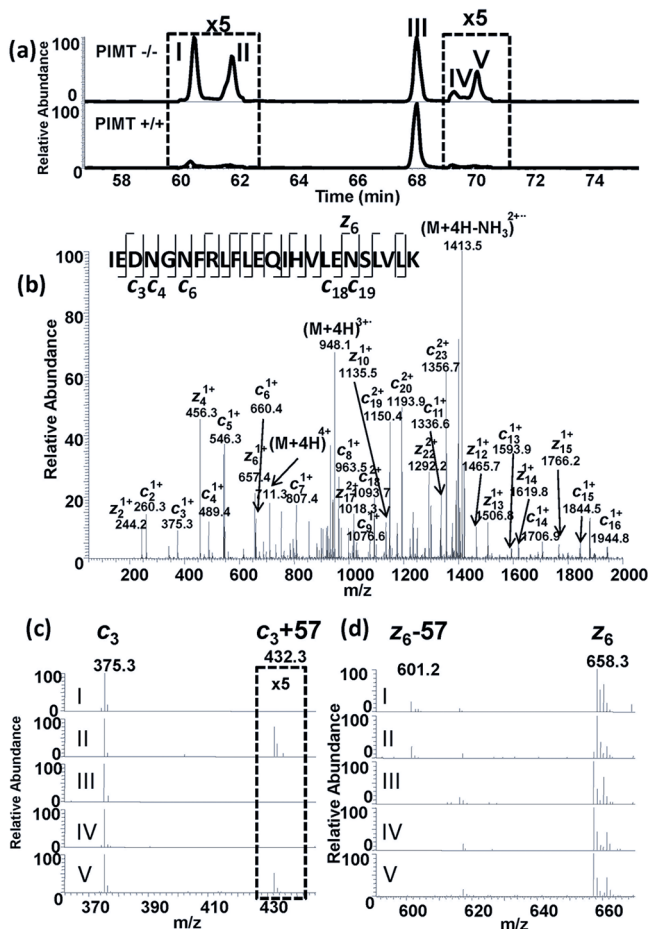
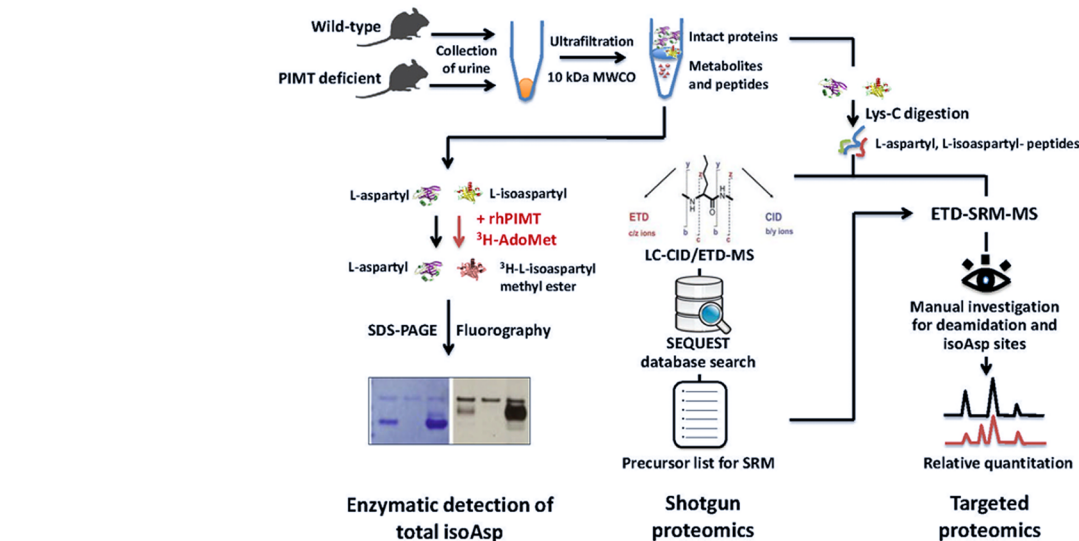


**Figure 2.** Extracted ion chromatograms and ETD spectra of MUP1 peptide (50–73), IE<sup>52</sup>D<sup>53</sup>NG<sup>55</sup>NFR<sup>56</sup>LFLEQIHVLE<sup>68</sup>NSLVLK. (a) Extracted ion chromatograms of MUP1 peptide and its isomers from wild type and PIMT-deficient mice; (b) ETD spectrum of native MUP1 peptide (50–73); (c,d) reporter ions of isoAsp ( $c_3 + 57$ ,  $z_6 - 57$ ) in ETD MS/MS spectra from the selected precursors of above peptide and its isoaspartyl isoforms.

and Asp isoforms, which share high similarity of ETD MS/MS spectra.

Furthermore, the ETD-SRM method was optimized to increase the efficiency of ETD fragmentation for isoAsp analysis, in order to maximize the intensity of c and z product ions, including the specific reporter ions of isoAsp residues (the pair of  $c_{l-n} + 57$  and  $z_n - 57$  ions). First, we utilized the decision tree algorithm<sup>47</sup> to select precursor ions with relatively high intensity. The measured masses ranging at 650–950 ( $m/z$ ) and at least triply charged were the preferred candidate precursor ions for ETD fragmentation. Second, supplemental activation was implemented to enhance ETD fragmentation of doubly charged precursors.<sup>48</sup> Third, an isolation width at  $\pm 1.5$  Da/e for the ETD-SRM method was selected for the multiply charged precursor ions, allowing the inclusion of precursor ions of isoforms with at least 3 deamidated Asn residues in one peptide. The candidate peptides and their precursor ions ( $m/z$ ) and charge states are listed in Table SI-2 in the Supporting Information.

One targeted peptide, the MUP1 peptide (IEDNGNFR-LFLEQIHVLENSLVLK, 50–73; also shared with MUP6 and MUP8), containing four potential Asn deamidation and aspartyl isomerization sites, can serve to illustrate the data interpretation for identifying the isoAsp site(s). As shown in Figure 1 and Figure SI-1 in the Supporting Information, database searching resulted in 5 forms of the MUP1 peptide: the native form (peak III) and its four-deamidated isoforms (peaks I, II, IV, and V). To increase the confidence of isoAsp site mapping, multiple criteria were implemented for manual investigation, particularly, the unique reporter ions (the pair of  $c_{l-n} + 57$  and  $z_n - 57$  ions, the loss of 60.0 Da from the reduced species for Asp form) from more selective SRM scans. In brief, based on a +0.984 Da mass shift (from Asn to Asp or isoAsp) in the precursor ions, the peaks I, IV, and V were identified as monodeamidated forms of the peptide and a +1.968 Da mass shift for peak II as a dideamidated product. Further investigation of the ETD spectra and XICs revealed that peak I contained a deamidated modification of Asn68 to isoAsp68, according to the +0.984 Da mass shift. With the same approach, peaks IV and V were identified with the deamidation from Asn53 to Asp53 and isoAsp53, respectively. Peak II had the simultaneous deamidation sites of Asn53 to isoAsp53 and Asn68 to isoAsp68.

Table 1. Identification and Quantitation of isoAsp Peptides in MUPs

sequences and modifications	$\Delta$ mass (Da)	relative amount (%)		fold change (KO/WT) <sup>a</sup>
		KO	WT	
IED <sup>52</sup> N <sup>53</sup> GN <sup>55</sup> FRLFLEQIHVLEN <sup>68</sup> SLVLK, MUP1(50–73), also shared with MUP6 and MUP8				
Asn68 to isoAsp68	0.984	11.8	2.2	5.4
Asn53, Asn68 to isoAsp53, isoAsp68	1.968	12.0	2.2	5.4
native form	0.000	64.5	93.0	–1.4
Asn53 to Asp53	0.984	3.3	1.5	2.2
Asn53 to isoAsp53	0.984	8.4	1.1	7.6
HGILREN <sup>165</sup> IID <sup>168</sup> LSN <sup>171</sup> AN <sup>173</sup> RCLQARE, MUP1(159–180)				
Asn173 to isoAsp173	0.984	2.2	1.3	1.7
native form	0.000	92.6	93.4	1.0
Asn171 to Asp171	0.984	2.7	3.5	–1.3
Asn173 to Asp173	0.984	2.6	1.8	1.4
IED <sup>52</sup> N <sup>53</sup> GN <sup>55</sup> FRLFLEQIHVLEK, MUP2(50–68)				
Asn53 to Asp53	0.984	7.1	4.3	1.6
native form	0.000	60.4	68.9	–1.1
Asn53 to isoAsp53	0.984	32.5	26.7	1.2
IN <sup>34</sup> GEWHTIILASD <sup>45</sup> K, MUP1(33–46), also shared with MUP2, MUP6, and MUP8				
Asn34 to Asp34	0.984	6.0	3.1	1.9
native form	0.000	45.3	43.0	1.0
Asn34 to isoAsp34	0.984	48.7	53.9	–1.1

<sup>a</sup>Estimated fold change by dividing the peak area of each peptide isoform of PIMT-deficient mice by that of the wild type mice. The positive and negative values show the elevated and decreased level, respectively, in PIMT-deficient mice.

It is important to note that we found it a challenge to confidently identify all Asn deamidation and Asp isomerization sites in a proteome scale using conventional shotgun proteomics. The randomly selected MS/MS scans in a data-dependent mode would not ensure the fragmentation of precursor ions at the chromatographic peak apex, thus leading to lower sensitivity of detection and poor quality of MS/MS spectra. When the automated software was used for assignment of modification sites, these low-quality spectra could potentially result in a high false positive rate.<sup>36</sup> An example for such a challenge is demonstrated by the above peptide, MUP1 peptide (50–73). As shown in Figure 2, from the shotgun proteomics, the unmodified MUP1 peptide (50–73) (peak III) was identified from both WT and KO mice while its deamidated isoforms (either Asp or isoAsp or the combination of the two, peaks I, II, IV, and V) only from KO mice. The isoforms (peaks I, II, IV, and V) in relatively low abundances in wild type mice and their deamidation sites could not be confidently identified. In addition, the occurrence of isoaspartyl and aspartyl residues in deamidated peptides could not be differentiated. The implementation of targeted proteomics using the ETD-SRM method complemented the above limitation by providing enhanced sensitivity for detection and differentiating isoAsp and Asp, based on the unique ETD-fragment ions. For the above deamidated isoforms of MUP1 peptide (50–73), the specific isoAsp/Asp sites were assigned, with their relative abundance estimated at less than 3% of the total abundance in the urine of WT mice.

In total, of 38 putative isoAsp-containing sites from the 13 candidate MUP peptides, 6 Asn residues were found to be deamidated (5 confirmed to form isoAsp), as summarized in Table 1. The remaining 14 Asn residues were observed with no modification, and 18 Asp residues were found with no detectable isomerization. These findings revealed the isoAsp

sites that contribute to the elevated isoAsp level in MUP species in KO-male mouse urine. For the wild type mice, very low level of isoAsp was observed in urine, indicating that PIMT-catalyzed conversion from isoAsp to Asp is an efficient process.

**IsoAsp Formation during Sample Preparation.** As illustrated in Scheme 1, isoAsp is spontaneously generated from the deamidation of Asn or isomerization of Asp. Thus, isoAsp might occur during sample preparation. To examine the potential of this artifact, we conducted Lys-C digestion in <sup>18</sup>O-labeled water.<sup>25,26,49,50</sup> Under such conditions, deamidation products would contain <sup>18</sup>O, resulting in an increase of mass of 2 Da. Briefly, mice urine was treated at 37 °C and pH 8.3 overnight, stress conditions that are harsher than those for the sample analysis described above. Nonetheless, the “hot spot” NG sequence in two peptides, IEDNGNFRLFLEQIHVLEK and INGEWHTIILASDK generated only less than 5% and 3% of artificial deamidation products, respectively. No isoAsp was detected from the other asparaginyl and aspartyl residues during sample preparation. Thus a negligible level of artificial isoAsp was generated during our sample analysis.

**IsoAsp in MUPs from Wild Type and PIMT-Knockout Mice.** Once the candidate peptides were characterized, the precursor mass of the native forms and isoAsp counterparts were extracted and the XIC peak areas used for quantitation. Since various forms of a given peptide were observed in the same run, the estimated stoichiometry (ES, %) was used as a quantitative measure of the extent of deamidation and isomerization at each site, as utilized in a previous study.<sup>34</sup> Briefly, the estimated stoichiometry was obtained from the peak area of the measured individual isoform divided by the sum of all forms of the given peptide. As an example, the percentages of native MUP1 peptide (50–73), IEDNGNFRLFLEQIHVLENSLVLK, and the corresponding four deamidated

isoforms (isoAsp, Asp and the combination thereof) in the wild type and PIMT-deficient mice are shown in Figure 1 and Table 1. PIMT-deficient male mice urine showed a higher level of isoAsp than that of the wild type mice urine. As a particularly striking example, 8.4% of the isoAsp isoform, IED<sub>iso</sub>DGNFRL-FLEQIHVLENSLVK, in the PIMT-deficient mouse was found, compared to only 1.1% in the wild type mouse, a nearly 8-fold higher isoAsp level. As another example, a doubly modified isoAsp peptide, IED<sub>iso</sub>DGNFRLFLEQIHVL-EisoDSLVLK, had almost a 6-fold increase in PIMT knockout mice, relative to the wild type. As seen in Table 1, the relative quantitation analysis for other isoAsp-containing peptides also showed a trend of elevated level of deamidation-induced isoAsp in PIMT-deficient mice. The identification and quantitation of isoAsp sites will be important in a future study examining the molecular basis of the excretion processes.

## CONCLUSIONS

For the first time, both the secreted functional proteins (native MUPs) and excreted intact damaged proteins (deamidated and isoaspartyl-containing MUPs) in mouse urine have been systematically analyzed at the molecular level for their relative amount of isoAsp, protein identity, and sites of modifications. Our results strongly suggest that both excretion (intact isoAsp-proteins) and proteolysis (degraded isoAsp-peptides followed by excretion) are operative in the removal of isoAsp species from circulation in mice, in addition to the known repair process driven by the PIMT enzyme. From the analytical perspective, isoAsp posed unique technical challenges. The ETD-SRM targeted proteomics strategy has been shown to be particularly effective in providing confident identification of the sites of isoAsp/Asp and dramatically enhances the sensitivity of isoAsp detection and quantitation. The strategy developed here allows the monitoring of isoAsp in individual proteins and specific sites within, so that the proposed excretion and proteolysis pathways for isoaspartyl containing proteins can now be investigated at the molecular and sequence level. Moreover, our strategy is equally useful to examine isoAsp isoforms that are ubiquitous in protein pharmaceuticals and that accumulate during both storage and circulation.

## ASSOCIATED CONTENT

### Supporting Information

Additional information as noted in text. This material is available free of charge via the Internet at <http://pubs.acs.org>.

## AUTHOR INFORMATION

### Corresponding Author

\*B. L. Karger: e-mail, [b.karger@neu.edu](mailto:b.karger@neu.edu). Z. S. Zhou: e-mail, [z.zhou@neu.edu](mailto:z.zhou@neu.edu).

### Notes

The authors declare no competing financial interest.

## ACKNOWLEDGMENTS

This work was supported by NIH Grant GM101396 to Z.S.Z., Grant GM15847 to B.L.K., Grant GM026020 to S.G.C., and Grants GM007185 to A.N.P. (the Ruth L. Kirschstein National Research Service Award). The authors also thank Dr. Bruce Downie for providing a plasmid encoding the rhPIMT. This is contribution number 1025 from the Barnett Institute.

## REFERENCES

- (1) Geiger, T.; Clarke, S. *J. Biol. Chem.* **1987**, *262*, 785–94.
- (2) Robinson, N. E.; Robinson, A. B. *Proc. Natl. Acad. Sci. U.S.A.* **2001**, *98*, 12409–12413.
- (3) Shimizu, T.; Matsuoka, Y.; Shirasawa, T. *Biol. Pharm. Bull.* **2005**, *28*, 1590–1596.
- (4) Clarke, S. *Ageing Res. Rev.* **2003**, *2*, 263–285.
- (5) Furuchi, T.; Homma, H. *Yakugaku Zasshi* **2007**, *127*, 1927–1936.
- (6) Ota, I. M.; Clarke, S. *Biochemistry* **1989**, *28*, 4020–4027.
- (7) Najbauer, J.; Orpiszewski, J.; Aswad, D. W. *Biochemistry* **1996**, *35*, 5183–5190.
- (8) Roher, A. E.; Lowenson, J. D.; Clarke, S.; Wolkow, C.; Wang, R.; Cotter, R. J.; Reardon, I. M.; Zurcher-Neely, H. A.; Heinrikson, R. L.; Ball, M. J.; et al. *J. Biol. Chem.* **1993**, *268*, 3072–3083.
- (9) Sargaeva, N. P.; Lin, C.; O'Connor, P. B. *Anal. Chem.* **2009**, *81*, 9778–9786.
- (10) Doyle, H. A.; Gee, R. J.; Mamula, M. J. *Autoimmunity* **2007**, *40*, 131–137.
- (11) Cimmino, A.; Capasso, R.; Muller, F.; Sambri, I.; Masella, L.; Raimo, M.; De Bonis, M. L.; D'Angelo, S.; Zappia, V.; Galletti, P.; Ingrosso, D. *PLoS One* **2008**, *3*, e3258.
- (12) Liu, Y. D.; van Enk, J. Z.; Flynn, G. C. *Biologicals* **2009**, *37*, 313–322.
- (13) Paranandi, M. V.; Guzzetta, A. W.; Hancock, W. S.; Aswad, D. W. *J. Biol. Chem.* **1994**, *269*, 243–253.
- (14) Liu, H.; Gaza-Bulseco, G.; Sun, J. *J. Chromatogr., B: Anal. Technol. Biomed. Life Sci.* **2006**, *837*, 35–43.
- (15) Zhang, W.; Czupryn, M. J. *J. Pharm. Biomed. Anal.* **2003**, *30*, 1479–1490.
- (16) Cloos, P. A.; Christgau, S. *Biogerontology* **2004**, *5*, 139–158.
- (17) Carmel, R.; Jacobsen, D. W. *Homocysteine in Health and Disease*. Cambridge University Press: Cambridge, U.K., 2001; p xvi.
- (18) McFadden, P. N.; Clarke, S. *Proc. Natl. Acad. Sci. U.S.A.* **1987**, *84*, 2595–2599.
- (19) Chavoua, D. A.; Jackson, F. R.; O'Connor, C. M. *Proc. Natl. Acad. Sci. U.S.A.* **2001**, *98*, 14814–14818.
- (20) Kindrachuk, J.; Parent, J.; Davies, G. F.; Dinsmore, M.; Attah-Poku, S.; Napper, S. *J. Biol. Chem.* **2003**, *278*, 50880–50886.
- (21) Lee, B. W.; Sun, H. G.; Zang, T.; Kim, B. J.; Alfaro, J. F.; Zhou, Z. *J. Am. Chem. Soc.* **2010**, *132*, 3642–3643.
- (22) Lowenson, J. D.; Kim, E.; Young, S. G.; Clarke, S. *J. Biol. Chem.* **2001**, *276*, 20695–20702.
- (23) Cannon, L. M.; Butler, F. N.; Wan, W.; Zhou, Z. *S. Anal. Biochem.* **2002**, *308*, 358–363.
- (24) Vlasak, J.; Bussat, M. C.; Wang, S.; Wagner-Rousset, E.; Schaefer, M.; Klinguer-Hamour, C.; Kirchmeier, M.; Corvaia, N.; Ionescu, R.; Beck, A. *Anal. Biochem.* **2009**, *392*, 145–154.
- (25) Li, X.; Cournoyer, J. J.; Lin, C.; O'Connor, P. B. *J. Am. Soc. Mass Spectrom.* **2008**, *19*, 855–864.
- (26) Gaza-Bulseco, G.; Li, B.; Bulseco, A.; Liu, H. C. *Anal. Chem.* **2008**, *80*, 9491–9498.
- (27) Liu, M.; Cheetham, J.; Cauchon, N.; Ostovic, J.; Ni, W.; Ren, D.; Zhou, Z. *S. Anal. Chem.* **2012**, *84*, 1056–1062.
- (28) Alfaro, J. F.; Gillies, L. A.; Sun, H. G.; Dai, S.; Zang, T.; Klaene, J. J.; Kim, B. J.; Lowenson, J. D.; Clarke, S. G.; Karger, B. L.; Zhou, Z. *S. Anal. Chem.* **2008**, *80*, 3882–3889.
- (29) Murray, E. D., Jr.; Clarke, S. *J. Biol. Chem.* **1984**, *259*, 10722–10732.
- (30) Vigneswara, V.; Lowenson, J. D.; Powell, C. D.; Thakur, M.; Bailey, K.; Clarke, S.; Ray, D. E.; Carter, W. G. *J. Biol. Chem.* **2006**, *281*, 32619–32629.
- (31) Zhu, J. X.; Doyle, H. A.; Mamula, M. J.; Aswad, D. W. *J. Biol. Chem.* **2006**, *281*, 33802–33813.
- (32) Cournoyer, J. J.; Pittman, J. L.; Ivleva, V. B.; Fallows, E.; Waskell, L.; Costello, C. E.; O'Connor, P. B. *Protein Sci.* **2005**, *14*, 452–463.
- (33) O'Connor, P. B.; Cournoyer, J. J.; Pitteri, S. J.; Chrisman, P. A.; McLuckey, S. A. *J. Am. Soc. Mass Spectrom.* **2006**, *17*, 15–19.

- (34) Ni, W.; Dai, S.; Karger, B. L.; Zhou, Z. S. *Anal. Chem.* **2010**, *82*, 7485–7491.
- (35) Kim, M. S.; Pandey, A. *Proteomics* **2012**, *12*, 530–542.
- (36) Yang, H.; Fung, E. Y.; Zubarev, A. R.; Zubarev, R. A. *J. Proteome Res.* **2009**, *8*, 4615–4621.
- (37) Savitski, M. M.; Fischer, F.; Mathieson, T.; Sweetman, G.; Lang, M.; Bantscheff, M. *J. Am. Soc. Mass Spectrom.* **2010**, *21*, 1668–1679.
- (38) Kiyonami, R.; Schoen, A.; Prakash, A.; Peterman, S.; Zabrouskov, V.; Picotti, P.; Aebersold, R.; Huhmer, A.; Domon, B. *Mol. Cell. Proteomics* **2011**, *10*, M110 002931.
- (39) Kim, E.; Lowenson, J. D.; MacLaren, D. C.; Clarke, S.; Young, S. G. *Proc. Natl. Acad. Sci. U.S.A.* **1997**, *94*, 6132–6137.
- (40) Dinkins, R. D.; Majee, S. M.; Nayak, N. R.; Martin, D.; Xu, Q.; Belcastro, M. P.; Houtz, R. L.; Beach, C. M.; Downie, A. B. *Plant J.* **2008**, *55*, 1–13.
- (41) Elias, J. E.; Gygi, S. P. *Nat. Methods* **2007**, *4*, 207–214.
- (42) Pisitkun, T.; Johnstone, R.; Knepper, M. A. *Mol. Cell. Proteomics* **2006**, *5*, 1760–1771.
- (43) Shui, H. A.; Huang, T. H.; Ka, S. M.; Chen, P. H.; Lin, Y. F.; Chen, A. *Nephrol. Dial. Transplant.* **2008**, *23*, 176–185.
- (44) Hui, X.; Zhu, W.; Wang, Y.; Lam, K. S.; Zhang, J.; Wu, D.; Kraegen, E. W.; Li, Y.; Xu, A. *J. Biol. Chem.* **2009**, *284*, 14050–14057.
- (45) Armstrong, S. D.; Robertson, D. H.; Cheetham, S. A.; Hurst, J. L.; Beynon, R. J. *Biochem. J.* **2005**, *391*, 343–350.
- (46) Beynon, R. J.; Veggerby, C.; Payne, C. E.; Robertson, D. H.; Gaskell, S. J.; Humphries, R. E.; Hurst, J. L. *J. Chem. Ecol.* **2002**, *28*, 1429–1446.
- (47) Swaney, D. L.; McAlister, G. C.; Coon, J. J. *Nat. Methods* **2008**, *5*, 959–964.
- (48) Chan, W. Y.; Chan, T. W.; O'Connor, P. B. *J. Am. Soc. Mass Spectrom.* **2010**, *21*, 1012–1015.
- (49) Wang, Z.; Rejtar, T.; Zhou, Z. S.; Karger, B. L. *Rapid Commun. Mass Spectrom.* **2010**, *24*, 267–275.
- (50) Du, Y.; Wang, F.; May, K.; Xu, W.; Liu, H. *Anal. Chem.* **2012**, *84*, 6355–6360.

## Supporting Information

### **An Integrated Proteomic Analysis of Major Isoaspartyl-Containing Proteins in the Urine of Wild Type and Protein L-Isoaspartate *O*-Methyltransferase-Deficient Mice**

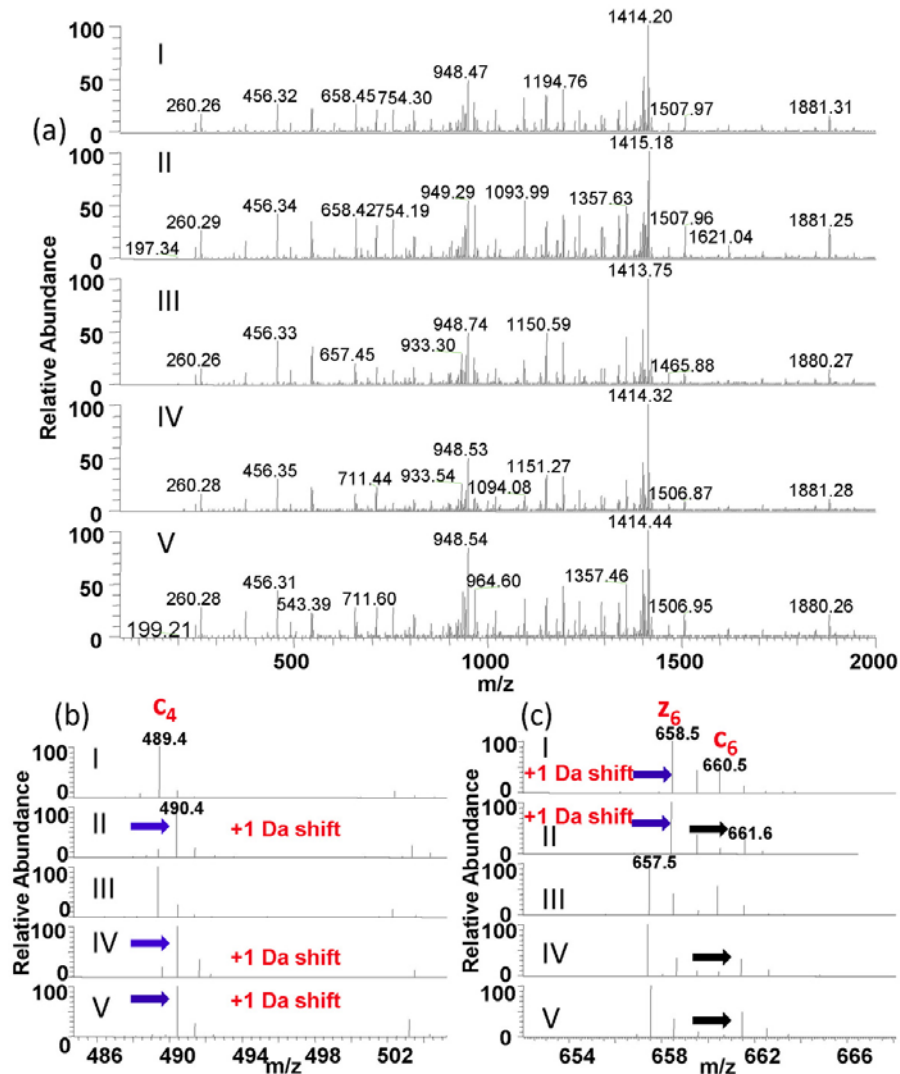
Shujia Dai<sup>1</sup>, Wenqin Ni<sup>1,2</sup>, Alexander N. Patananan<sup>3</sup>, Steven G. Clarke<sup>3</sup>, Barry L. Karger<sup>1,2\*</sup>, Zhaohui Sunny Zhou<sup>1,2,\*</sup>

1 Barnett Institute of Chemical and Biological Analysis, Northeastern University, Boston MA 02115

2 Department of Chemistry and Chemical Biology, Northeastern University, Boston MA 02115

3 Department of Chemistry and Biochemistry and the Molecular Biology Institute, UCLA, Los Angeles, CA 90095

\* To whom correspondence should be addressed. B.L. Karger: e-mail, [b.karger@neu.edu](mailto:b.karger@neu.edu); Z.S. Zhou: e-mail, [z.zhou@neu.edu](mailto:z.zhou@neu.edu).



34

35 **Figure SI-1. Examination of isoAsp sites in MUP1 peptide (50-73).** (a) ETD spectrum of  
 36 peptide IED<sup>52</sup>N<sup>53</sup>GN<sup>55</sup>FRLFLEQIHVLEN<sup>68</sup>SLVLK and its isomers from MUP2; (b and c) the  
 37 expanded ETD spectra of the peptide IED<sup>52</sup>N<sup>53</sup>GN<sup>55</sup>FRLFLEQIHVLEN<sup>68</sup>SLVLK and its  
 38 isomers, leading to the identification of deamidation sites.

39 **Table SI-1. Identified proteins (>2 distinct peptides) in mouse urine by discovery**40 **proteomics.**

SwissProt Accession	Description	Protein Symbol	M.W. /kDa	Sequence Coverage	Distinct Peptides	Spectral counts
P11588	Major urinary protein 1	MUP1	20.6	91.4	15	1373
P11589	Major urinary protein 2	MUP2	20.7	88.3	13	1331
P02762	Major urinary protein 6	MUP6	20.6	91.4	12	1287
P04938	Major urinary proteins 11 and 8	MUP8	17.5	98.0	12	1287
P04939	Major urinary protein 3	MUP3	21.5	54.3	5	77
P15947	Kallikrein-1	KLK1	28.8	39.9	8	28
Q61207	Sulfated glycoprotein 1	SAP	61.4	12.8	6	27
P01132	Pro-epidermal growth factor	EGF	133.1	12.4	7	17
P35459	Lymphocyte antigen 6D	LY6D	13.4	22.1	2	16
P07724	Serum albumin	ALBU	68.6	19.9	7	15
P15945	Kallikrein 1-related peptidase b5	K1KB5	28.7	10.3	4	11
P28825	Meprin A subunit alpha	MEP1A	84.1	11.7	5	11
P28798	Granulins	GRN	63.4	11.0	3	9
Q9DAU7	WAP four-disulfide core domain protein 2	WFDC2	18.0	27.0	3	9
P15501	Prostatic spermine-binding protein	SPBP	22.0	14.1	2	8
Q8BZH1	Protein-glutamine gamma-glutamyltransferase 4	TGM4	75.5	16.3	8	8
P09803	Cadherin-1	CADH1	98.2	8.4	4	6
Q06890	Clusterin	CLUS	51.6	8.7	3	6
P08228	Superoxide dismutase [Cu-Zn]	SODC	15.9	24.7	2	6
P10923	Osteopontin	OSTP	32.4	15.0	2	4
Q9WTR5	Cadherin-13	CAD13	78.2	3.1	2	3
P06281	Renin-1	RENI1	44.3	6.2	2	3
P00796	Renin-2	RENI2	44.3	6.2	2	3
P56480	ATP synthase subunit beta, mitochondrial	ATPB	56.3	4.4	2	2
P49183	Deoxyribonuclease-1	DNAS1	32.0	16.6	2	2
Q02596	Glycosylation-dependent cell adhesion molecule 1	GLCM1	16.2	21.2	2	2

41

42

43 **Table SI-2. Selected candidates for targeted ETD-SRM detection.** The investigated sites are  
 44 underlined. The listed peptides containing potential isoAsp were selected for targeted ETD-  
 45 SRM.

<b>Sequences</b>	<b>Proteins</b>	<b><i>m/z</i></b>	<b><i>z</i></b>
IED <u>NG</u> N <u>FRL</u> FLEQIHVLEK	MUP2	772.1	3
HGILRE <u>NI</u> I <u>DLS</u> N <u>ANR</u> CLQARE	MUP1	648.8	4
I <u>NGE</u> WHTIILAS <u>DK</u>	MUP1, 2, 6, 8	533.0	3
IED <u>NG</u> N <u>FRL</u> FLEQIHVLE <u>NSL</u> VLK	MUP1	710.9	4
T <u>DYD</u> N <u>FL</u> MAH <u>LIN</u> EK	MUP1, 2, 6, 8	608.6	3
AGIYYM <u>NYD</u> GF <u>N</u> TFSILK	MUP3	1059.0	2
AGEYSV <u>TYD</u> GF <u>N</u> TFTIPK	MUP1, 2, 6, 8	670.7	3
<u>DGET</u> F <u>QLM</u> GLYGRE <u>PDL</u> SS <u>DIK</u>	MUP1, 2, 6, 8	824.4	3
FHTVR <u>DEE</u> CSELSM <u>VAD</u> K	MUP1, 2, 6, 8	718.3	3
FHLIV <u>NEE</u> CTEMTAIGE <u>QTEK</u>	MUP3	827.1	3
TF <u>QLM</u> E <u>LYG</u> REP <u>DLSL</u> DIK	MUP3	756.7	3
LCEEHGI <u>IRE</u> NI <u>IDL</u> T <u>NV</u> NR <u>CLE</u> ARE	MUP3	792.4	4
T <u>DYD</u> NYIM <u>IHL</u> IN <u>K</u>	MUP3	876.9	3

46

47